

Special Issue of the 6th International Congress & Exhibition (APMAS2016), Maslak, Istanbul, Turkey, June 1–3, 2016

Characterization of Nd and Sm Co-Doped CeO₂-Based Systems

A. ARABACI^{a,*}, M. DER^b, M.F. ÖKSÜZÖMER^b AND T.G. ALTINÇEKİÇ^b

^aIstanbul University, Faculty of Engineering, Department of Metallurgical and Materials Engineering, 34320 Istanbul, Turkey

^bIstanbul University, Faculty of Engineering, Department of Chemical Engineering, 34320 Istanbul, Turkey

Nd_{0.20}Sm_xCe_{0.8-x}O_{1.9-x/2} ($x = 0, 0.05, 0.10, 0.15, 0.20$) rare-earth-co-doped ceria electrolytes were synthesized by polyol process. Acetate compounds of cerium and dopants (Nd, Sm) were used as starting materials and triethylene glycol was used as a solvent. Structural and ionic conductivity properties of the electrolyte systems were determined by applying characterization techniques such as X-ray diffraction, the Fourier transform infrared spectroscopy, scanning electron microscope, and electrochemical impedance spectroscopy. The results of X-ray diffraction indicated that a single-phase fluorite structure formed at the relatively low calcination temperature of 600 °C. So, the samples were calcined at 600 °C for 4 h and then sintered at 1400 °C for 6 h to obtain dense ceramics (between 85 and 90%). The two-probe ac impedance spectroscopy was used to study the total ionic conductivity of doped and co-doped ceria samples. The results of the impedance spectroscopy indicate that the Nd_{0.20}Sm_{0.05}Ce_{0.75}O_{1.875} composition exhibited highest ionic conductivity value, 3.60×10^{-2} S cm⁻¹ at 800 °C.

DOI: [10.12693/APhysPolA.131.78](https://doi.org/10.12693/APhysPolA.131.78)

PACS/topics: 88.30.pn

1. Introduction

Solid oxide fuel cells (SOFCs) are the most efficient devices yet invented for conversion of chemical fuels directly into electrical power [1]. A fuel cell consists of an anode, a cathode, and an electrolyte. Commonly, stabilized zirconia (e.g. yttria stabilized zirconia), doped ceria (e.g. samaria doped or gadolinia doped ceria), stabilized Bi₂O₃ and strontium doped lanthanum gallate are used as electrolyte materials for SOFC applications. A typical SOFC which uses yttria stabilized zirconia (YSZ) as the electrolyte requires high operation temperature (1000 °C) to achieve sufficient ionic conductivity [2]. Such a high operation temperature required for YSZ can cause technological problems, such as mechanical instability, reduced lifetime and undesirable reactions between the cell components (electrolyte, electrodes, and interconnecting materials) [3, 4]. For this reason, reducing the operation temperature of SOFCs is important for achieving long-term performance stability and for reducing the cost of materials processing and cell fabrication. To reduce the operation temperature, alternative electrolyte materials with higher conductivity at lower temperatures should be developed. Doped ceria electrolytes showed higher ionic conductivities at relatively low operation temperatures, < 800 °C. In comparison to that of YSZ and ceria doped with heterovalent cations, such as rare earth and alkaline earth ions have been extensively studied as the most promising electrolyte materials for intermediate temperature solid oxide fuel cells (IT-SOFC) [3]. As reported in the

previous studies [5–7], co-doping could enhance the ionic conductivity. Dopant ion, dopant concentration, oxygen vacancy concentration and local defect structure are the factors, which can influence the total ionic conductivity in doped CeO₂ [8, 9].

To obtain pure doped CeO₂ powders, various techniques have been used such as citric-nitrate combustion [6] and sol-gel method [5, 8], etc. Among these techniques, polyol method, which is generally used for producing metallic particles, could be employed to synthesize metal oxide particles. The basis of this method is the precipitation of solid materials while heating the suitable precursors in a multivalent and high-boiling point alcohol such as triethylene glycol (TREG). The alcohol acts as a stabilizer, also limiting particle growth and prohibiting agglomeration [10]. Materials, obtained from this method, show homogeneous phase composition, narrow particle size distribution, and high specific surface area. Also the morphology could be controlled by changing the reaction time and the concentration of the precursor [11]. In our previous work [12] we investigated Ce_{1-x}RE_xO_{2-x/2} (RE = Sm, Gd, Nd, La) at varying dopant concentrations ($x = 0.05-0.25$) by using the polyol method for IT-SOFCs.

In the present work, in order to develop intermediate temperature electrolyte material for SOFC, Sm³⁺ and Nd³⁺ co-doped ceria based materials Nd_{0.20}Sm_xCe_{0.8-x}O_{1.9-x/2} ($x = 0, 0.05, 0.10, 0.15, 0.20$) were prepared and characterized. Effects of co-doping on the structure and electrical conductivity were studied in comparison with the neodymium-doped ceria, Nd_{0.20}Ce_{0.80}O_{1.90}, in the temperature range of 300–800 °C. Effects of co-doping and the doping content for the ceria co-doped with Sm³⁺ and Nd³⁺ were investigated.

*corresponding author; e-mail: aliye@istanbul.edu.tr

2. Material and method

Nd_{0.20}Sm_xCe_{0.8-x}O_{1.9-x/2} ($x = 0, 0.05, 0.10, 0.15, 0.20$) solid solutions were synthesized by the polyol process using cerium acetate hydrate, neodymium acetate hydrate, and samarium acetate hydrate as the starting materials. Details about the polyol process were reported in our previous work [12]. X-ray diffraction (XRD) technique was used to identify the crystalline structure, phase purity, and lattice parameters of the powders. Calcined powders were analyzed by XRD technique using a Rigaku D/max-2200 Ultima X-ray diffractometer with Cu K_{α} radiation (0.15418 nm) in an angular region of $2\theta = 10\text{--}90^{\circ}$. The average crystallite sizes of the calcined powders were calculated from the X-ray line broadening of the reflections of (111) by using the well-known Scherrer equation [12]. The calcined powders were pressed into disc shaped pellets at 200 MPa with CIP. The compact disc pellets of the doped ceria powders were then sintered at 1400 °C for 6 h. The lattice parameters of the sintered samples were calculated by using the relations

$$a = d\sqrt{h^2 + k^2 + l^2}, \quad (1)$$

$$d = \frac{\lambda}{2 \sin \theta} \quad (2)$$

where d is the planar spacing, λ is the wavelength of the radiation, θ is the diffraction angle, and a is the lattice parameter which is calculated by the Bragg law and h , k , and l are the Miller indices of the plane. Infrared spectra of the calcined and sintered powders were recorded in the range of 350–4000 cm⁻¹, using a Fourier transform infrared spectrometer (Spectrum 100, Perkin Elmer). The densities of the sintered pellets were measured by the well-known Archimedes method [12]. The microstructure of the sintered samples were investigated by FEI Quanta FEG scanning electron microscope. The ionic conductivity values of the sintered samples were measured with an ac impedance analyzer (Solartron 1260 FRA and 1296 interface) in the temperature range of 300–800 °C. The Arrhenius plots were formed, and activation energies were calculated as Eq. (3):

$$\sigma = \frac{\sigma_0}{T} e^{-E_a/kT}, \quad (3)$$

where E_a is the activation energy, T is the absolute temperature, k is the Boltzmann constant, σ is the ionic conductivity and σ_0 is a preexponential factor. The total resistance of samples, R_t , can be obtained from impedance spectroscopy at different temperatures. The total ionic conductivity (σ) values were then calculated by using the equation of $\sigma = l/AR_t$ where R_t is the total resistance, l is the thickness and A is the cross-sectional area of the sample.

3. Results and discussion

Figure 1a and b shows the XRD patterns of the calcined and sintered Nd_{0.20}Sm_xCe_{0.8-x}O_{1.9-x/2} ($x = 0, 0.05, 0.10, 0.15, 0.20$) series, respectively. These results indicate that all of the synthesized samples are cubic fluorite structure of single phase CeO₂ (JCPDS Card

No: 34-394) and no other secondary phase was observed. Also, the dopant ions were fully substituted in the ceria lattice.

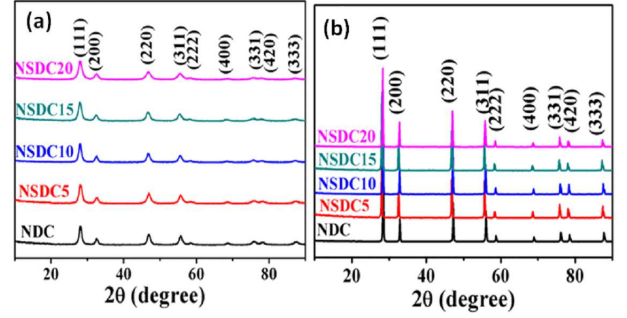


Fig. 1. XRD patterns of intensity for all samples after calcination (a) and sintering (b) (NDC = Nd_{0.20}Ce_{0.80}O_{1.90}, NSDC5 = Nd_{0.20}Sm_{0.05}Ce_{0.75}O_{1.875}, NSDC10 = Nd_{0.20}Sm_{0.10}Ce_{0.70}O_{1.850}, NSDC15 = Nd_{0.20}Sm_{0.15}Ce_{0.65}O_{1.825}, NSDC20 = Nd_{0.20}Sm_{0.20}Ce_{0.60}O_{1.80}).

The average crystallite sizes of the rare-earth-co-doped ceria powders after heat treatment at 600 °C were calculated between 7.3 and 10.4 nm. The lattice parameters were determined by using the XRD data of the sintered samples. When the dopant cation (Sm³⁺) was introduced to the structure, the lattice parameters increased relatively to the dopant concentration. This may be due to difference in ionic radii of Ce⁴⁺, Sm³⁺, and Nd³⁺ ($r_{Nd} > r_{Sm} > r_{Ce}$) [13]. The introduction of Nd³⁺ and Sm³⁺ into Ce⁴⁺ can cause a small shift in the ceria peaks. This shift is indicative of the change in the lattice parameter. As the Sm content increases, the lattice parameter increases for the Nd_{0.20}Sm_xCe_{0.8-x}O_{1.9-x/2} ($x = 0, 0.05, 0.10, 0.15$) samples. Figure 2 reports the Fourier transform infrared (FTIR) spectra of the calcined Nd_{0.20}Sm_xCe_{0.8-x}O_{1.9-x/2} samples. FTIR analysis shows that the strong peaks that belong to the Me–O bond were observed remarkably between 700 and 400 cm⁻¹. The weak band between 3600 and 3200 cm⁻¹ due to the O–H stretching vibration was attributed to water [14].

Figure 3 shows the SEM micrographs of the sintered pellets. The SEM images exhibited a dense structure and grain size in the range of 1.0–1.6 μm. The sintered samples have values between 85 and 90% of the relative density.

In this paper, the conductivity measured in air atmosphere can be described as the oxygen ion conductivity. The increase in ionic conductivities may be due to the increase in the oxygen vacancy concentration. The relationships between the dopant concentration and ionic conductivity are given in Table I. As can be seen from Table I, co-doped samples, Nd_{0.20}Sm_{0.05}Ce_{0.75}O_{1.875}, Nd_{0.20}Sm_{0.10}Ce_{0.70}O_{1.850}, showed apparently higher conductivities than the singly doped sample, Nd_{0.20}Ce_{0.80}O_{1.90}. This result demonstrates the existence of the co-doping effect. However, the

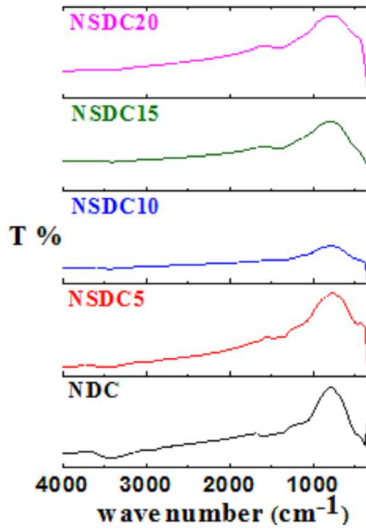


Fig. 2. FTIR transmission spectra of calcined $\text{Nd}_{0.20}\text{Sm}_x\text{Ce}_{0.8-x}\text{O}_{1.9-x/2}$ powders.

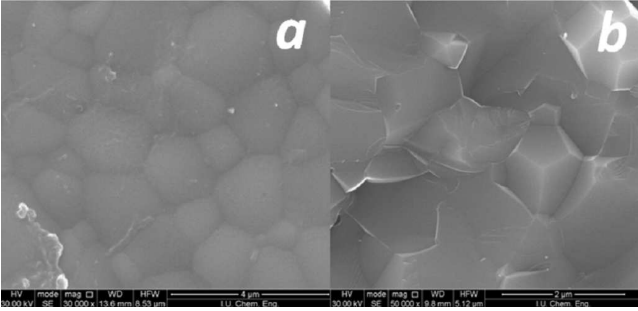


Fig. 3. SEM images of $\text{Nd}_{0.20}\text{Sm}_{0.05}\text{Ce}_{0.75}\text{O}_{1.875}$ sample sintered at $1400\text{ }^\circ\text{C}$ (a) from surface ($30,000\times$) and (b) from cross-section ($50,000\times$).

ionic conductivity values of $\text{Nd}_{0.20}\text{Sm}_{0.15}\text{Ce}_{0.65}\text{O}_{1.825}$, $\text{Nd}_{0.20}\text{Sm}_{0.20}\text{Ce}_{0.60}\text{O}_{1.80}$ samples are lower than the single doped ($x = 0$) ceria ($\text{Nd}_{0.20}\text{Ce}_{0.80}\text{O}_{1.90}$). The reason of this situation might be the ionic conductivity of the doped ceria which is related to the lattice distortion [9, 3]. As shown in Table I, the lattice constant of $\text{Nd}_{0.20}\text{Sm}_x\text{Ce}_{0.8-x}\text{O}_{1.9-x/2}$ increased with x . The $\text{Nd}_{0.20}\text{Sm}_{0.05}\text{Ce}_{0.75}\text{O}_{1.875}$ electrolyte material exhibited the highest ionic conductivity value at $800\text{ }^\circ\text{C}$ ($3.60 \times 10^{-2}\text{ S cm}^{-1}$). The conductivity results, which are comparable with the literature, were obtained [15, 16].

Figure 4 shows the Arrhenius plots for total ionic conductivity of electrolytes. The activation energy is minimum (0.79 eV) for the $\text{Nd}_{0.20}\text{Sm}_{0.05}\text{Ce}_{0.75}\text{O}_{1.875}$ sample between co-doped electrolytes (Table I). The decrease in activation energy may be due to the presence of attractive interactions between dopant cations and oxygen vacancies [3, 9]. Further, an increase in the Sm dopant content for $\text{Nd}_{0.20}\text{Sm}_x\text{Ce}_{0.8-x}\text{O}_{1.9-x/2}$ ($x = 0, 0.05, 0.10, 0.15, 0.20$) system, co-dopant prevents oxygen-ordering leading

TABLE I

Lattice parameter, ionic conductivity at $800\text{ }^\circ\text{C}$ and activation energies of samples for both low temperature and high temperature regimes

| x | α [Å] | σ at $800\text{ }^\circ\text{C}$ [S cm^{-1}] | E_a [eV] |
|------|--------------|--|------------|
| 0 | 5.444 | 2.84×10^{-2} | 0.80 |
| 0.05 | 5.459 | 3.60×10^{-2} | 0.79 |
| 0.10 | 5.461 | 3.03×10^{-2} | 0.93 |
| 0.15 | 5.467 | 1.95×10^{-2} | 1.00 |
| 0.20 | 5.463 | 2.13×10^{-2} | 1.11 |

to an increase in activation energy and a decrease in ionic conductivity in ceria solid solutions.

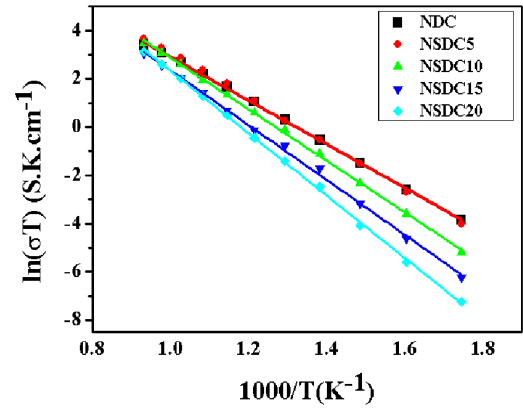


Fig. 4. Arrhenius plots of $\text{Nd}_{0.20}\text{Sm}_x\text{Ce}_{0.8-x}\text{O}_{1.9-x/2}$ systems. (NDC = $\text{Nd}_{0.20}\text{Ce}_{0.80}\text{O}_{1.90}$, NSDC5 = $\text{Nd}_{0.20}\text{Sm}_{0.05}\text{Ce}_{0.75}\text{O}_{1.875}$, NSDC10 = $\text{Nd}_{0.20}\text{Sm}_{0.10}\text{Ce}_{0.70}\text{O}_{1.850}$, NSDC15 = $\text{Nd}_{0.20}\text{Sm}_{0.15}\text{Ce}_{0.65}\text{O}_{1.825}$, NSDC20 = $\text{Nd}_{0.20}\text{Sm}_{0.20}\text{Ce}_{0.60}\text{O}_{1.80}$).

4. Conclusion

$\text{Nd}_{0.20}\text{Sm}_x\text{Ce}_{0.8-x}\text{O}_{1.9-x/2}$ ($x = 0, 0.05, 0.10, 0.15, 0.20$) rare-earth-co-doped ceria electrolytes were synthesized by using the polyol method. XRD results show that the doped ceria samples are all solid solutions of fluorite type structures that were formed in the calcination process and crystallized better in the sintering process. According to the electrochemical impedance spectroscopy results, the co-doped ceria of $\text{Nd}_{0.20}\text{Sm}_{0.05}\text{Ce}_{0.75}\text{O}_{1.875}$, $\text{Nd}_{0.20}\text{Sm}_{0.10}\text{Ce}_{0.70}\text{O}_{1.870}$, exhibited much higher ionic conductivities than that of the singly doped ceria ($\text{Nd}_{0.20}\text{Ce}_{0.80}\text{O}_{1.90}$) at $300\text{--}800\text{ }^\circ\text{C}$. As compared to other production techniques, the polyol method might be a good candidate for obtaining pure $\text{Nd}_{0.20}\text{Sm}_x\text{Ce}_{0.8-x}\text{O}_{1.9-x/2}$ phase for SOFC electrolyte applications.

Acknowledgments

This research work was supported by the Scientific and Technological Research Council of Turkey (TÜBİTAK), grant No. MAG-114M238, Research Fund of the Istanbul University, project No. 58111.

References

- [1] R.C. Biswal, K. Biswas, *Int. J. Hydrogen En.* **40**, 509 (2015).
- [2] A. Gondolini, E. Mercadelli, A. Sanson, S. Albonetti, L. Doubova, S. Boldrini, *J. Eur. Ceram. Soc.* **33**, 67 (2013).
- [3] H. Inaba, H. Tagawa, *Solid State Ion.* **83**, 1 (1996).
- [4] J.A. Kilner, *Solid State Ion.* **129**, 13 (2000).
- [5] S. Ramesh, V.P. Kumar, P. Kistaiah, C. Vishnuvardhan Reddy, *Solid State Ion.* **181**, 86 (2010).
- [6] Y. Liu, B. Li, X. Wei, W.J. Pan, *J. Am. Ceram. Soc.* **91**, 3926 (2008).
- [7] Y.F. Zheng, H.T. Gu, H. Chen, L. Gao, X.F. Zhu, L.C. Guo, *Mater. Res. Bull.* **44**, 775 (2009).
- [8] H. Yoshida, T. Inagaki, K. Miura, M. Inaba, Z. Ogumi, *Solid State Ion.* **160**, 109 (2003).
- [9] B.C.H. Steele, *Solid State Ion.* **129**, 95 (2000).
- [10] S.H. Ng, D.I. dos Santos, S.Y. Chew, D. Wexler, J. Wang, S.X. Dou, H.K. Liu, *Electrochem. Commun.* **9**, 915 (2007).
- [11] C. Ho, J.C. Yu, T. Kwong, A.C. Mak, S. Lai, *Chem. Mater.* **17**, 4514 (2005).
- [12] G. Dönmez, V. Sarıboğa, T.G. Altınçekiç, M.A.F. Öksüzömer, *J. Am. Ceram. Soc.* **98**, 501 (2015).
- [13] S. Ramesh, G. Upender, K.C.J. Raju, G. Padmaja, S.M. Reddy, C.V. Reddy, *J. Mod. Phys.* **4**, 859 (2013).
- [14] D. Maity, S.N. Kale, R. Kaul-Ghanekar, J. Xue, J. Ding, *J. Magn. Magn. Mater.* **321**, 3093 (2009).
- [15] F.Y. Wang, S. Chen, S. Cheng, *Electrochem. Commun.* **6**, 743 (2004).
- [16] S. Dikmen, H. Aslanbay, E. Dikmen, O. Sahin, *J. Power Sources* **195**, 2488 (2010).